Applied Mechanics and Materials
ISSN: 1662-7482, Vol. 750, pp 236-243
doi:10.4028/www.scientific.net/AMM.750.236

Submitted: 2014-10-01
Accepted: 2014-12-08
Online: 2015-04-15

Residual Stress Analysis for Engine Block by the Grooving Method

Chong Guo[1,a], Qinghua Lu[1,2,b*], Peilei Zhang[1,2,c], Birong Peng[1,d], Xiaofeng He[1,e]

[1] Shanghai University of Engineering Science, Shanghai City, China

[2] Shanghai Research & Development Center for Key Technologies of Intelligent Equipments of Ultra-Intense Laser Processing, Shanghai City, China

[a]guochong@sues.edu.cn, [b*]luqh@sues.edu.cn, [c]oxidpl@126.com, [d]335835906@qq.com, [e]534824181@qq.com

Keywords: engine block; residual stress; grooving method.

Abstract. The study of residual stress in engine block has the potential to provide the necessary infrastructure for a wide range of scientific and technological developments concerning the automobile industry. Such study can act as centre of excellence for scientific studies in the field of materials science and machinery as well as for industrial applications. The basic principle of measuring residual stress with grooving method and the main measuring steps were introduced in this paper. Groove cutting in the internal surface of engine block surrounds a given area in which the remaining stress is released, and then the strain results are recorded through strain gauge. The residual stress test data were compared at different positions of each engine block. It is found that engine blocks A and D on the sides of engine develop higher residual stresses than blocks B and C in the centre of engine. The stresses can be higher than 200MPa in tension in engine block A, depending on the geometry, size, microstructure, subsequent welding process, and cutting sequence. In addition, residual stress at the bottom of engine is higher than that at the top because of the structure of the engine. The residual stress is also calculated by numerical modeling method from which it shown that the condition is commendably fit the results which the distribution of stress.

1. Introduction

With the current demands of reducing automobile weight for improving fuel efficiency, cast aluminum are increasingly being used in automotive components including engine blocks, cylinder heads, intake manifolds, brackets, housings, chassis, transmission parts, and suspension systems[1]. As many of these applications involve cyclic loading, residual stress of the alloys are critical to their success. Because of the existence of residual stress, there will be a great drop in the strength of work piece occurred with defective workmanship like deformation and craze[2]. On the other hand, there is also change in dimensions of work piece and drop in mechanical properties such as fatigue strength and stress corrosion[3]. So this experiment is conducted on measuring remaining stresses and analyzing influence factor made by it to make sure the security and reliability of cylinder.

Castings made from aluminum alloys suffer contractions from solidification ranging from 4 to 7% that can cause dimensional distortion, hot tearing, porosities and the development of residual stresses[4]. The main cause for residual stresses in castings is the difference in solidification and cooling rates to which sections of different thickness are subjected; if the stresses are high enough they can promote the failure of an otherwise healthy piece[5]. Residual stresses may be reduced or eliminated by annealing, by plastic deformation or just by letting the piece at room temperature for enough time[6].

Usually there are two ways of testing welding residual stress to be known as mechanical release method and non-destructive method separately. The principle of the former is that using elasticity theory to measure the position possessed residual stress and separated from the work piece by machining operation, such as drill-hole method[7], cut emulated method[8] and ring-core method[9]. Compare with the former, the residual stress is obtained by the change of physical property caused by stress putting on the work piece, for instance, x-ray diffraction method[10, 11], neutron diffraction technique[12], magnetic method[13] and ultrasonic method[14]. Considering the complex construction inside the cylinder block, a special way to measure the stress is needed to solve the issue that whether it could be operable appropriately.

Against this background, a new way called grooving method was used to characterize residual stresses along inwall side of the cast engine block. The strains were measured both in top and bottom of cylinder in hoop, radial and axial orientations. Certainly the stresses were subsequently determined using generalized Hooke's law. Strain gauges correlate the change in electric resistance (R) of a metal deformed to a given value of strain (ε)[15]:

$$\frac{dR}{R} = S\varepsilon \,. \tag{1}$$

where S is the sensitivity of the gauge.

Using of aluminum has increased in automobiles to reduce weight and fuel consumption without impairing performance or safety for the occupants. An example is the substitution grey iron engine blocks by high performance aluminum alloys[16]. But cylinder liners in most engine blocks are of wear resistant castings made from prelatic irons. In some cases the liners are cast-in and generate residual stresses in the surrounding cylinder bridges[17].

2. Measuring method

2.1 principle of the grooving method

A way called grooving method is introduced to measure the remaining stress of cylinder. Grooves cut on the internal work piece's surface have surrounded a given area in which the remaining stress is released.

The remaining stress on the work piece's surface is σ_x, along x-direction and σ_y, alone y-direction respectively. The corresponding strain ε_x and ε_y are given by:

$$\varepsilon_x = -\frac{\sigma_x}{E} + \mu\frac{\sigma_y}{E} \,. \tag{2}$$

$$\varepsilon_y = -\frac{\sigma_y}{E} + \mu\frac{\sigma_x}{E} \,. \tag{3}$$

where E is elasticity modulus; and μ is Poisson's ratio of material.

The second item on the left of formula (2) and (3) is additional strain made by removing working stress which is perpendicular to axial direction of the groove. According to formula (2) and (3), the residual stress σ_x and σ_y can be obtained by:

$$\sigma_x = -\frac{E}{1-\mu^2}(\varepsilon_x + \mu\varepsilon_y) \,. \tag{4}$$

$$\sigma_y = -\frac{E}{1-\mu^2}(\varepsilon_y + \mu\varepsilon_x) \,. \tag{5}$$

Three pieces of rectangular gage are adopted for this test, as shown in Fig. 1, there are strains ε_0, ε_{45} and ε_{90} respectively corresponding to 0^o, 45^o and 90^o. Principal stress are set as σ_1 and σ_2（$\sigma_1 > \sigma_2$）, there are:

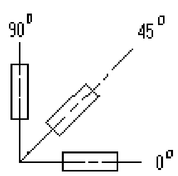

Fig. 1 Three pieces of rectangular rosette

$$\sigma_{1,2} = \frac{\mathrm{E}}{2}\left[\frac{\varepsilon_0 + \varepsilon_{90}}{1-\mu} \pm \frac{1}{1+\mu}\sqrt{(\varepsilon_0 - \varepsilon_{90})^2 + (2\varepsilon_{45} - \varepsilon_0 - \varepsilon_{90})^2}\right]. \tag{6}$$

3. Experimental process

3.1 Experimental materials

The cylinder material is A356 aluminum alloy which composition is shown in table 1. Due to the requirement of service performance the cast-iron HT250, as shown in table 2, is chosen as the material of cylinder sleeve which is fixed in aluminum alloy cylinder during the forming process. The physical dimension of aluminum alloy cylinder is 534mm in length, 389mm in width and 386mm in height. The maximum wall thickness of casting is about 20mm, on the contrary, the minimum thickness is about 4mm. the average wall thickness is about 8mm. It is a complex thick wall thickness casting. Its thermal conduction has an important effect on forming process and the quality of cast-parts[18].

Table 1 Composition of A356 aluminum alloy(*wt*%)

Si	Mg	Cu	Mn	Fe	Zn	Ti	Trace elements	Al
6.5~7.5	0.3	≤0.20	≤0.10	≤0.20	≤0.10	≤0.20	each≤0.15 total≤0.15	margin

Table 2 Composition of cast iron HT250(*wt*%)

C	Si	Mn	Gu	P	S	Fe
3.00~3.50	2.20~2.80	0.50~1.00	0.20~0.50	0.10~0.40	0.06~0.12	Margin

3.2 Experimental method

Planer tool is used for grooving inside the cylinder block, and the following points are the reference of opting measuring point's position:

(1) Operability and measurability;
(2) The possibly maximum residual stress at the casting solidification process;
(3) The maximum operating stress of finite element analysis;
(4) Parts of the fault location when process engine test and site test;
(5) Junction of cross section in heavy castings;
(6) The maximum cold forming position;
(7) Surface stress of machining area after process;
(8) Positions that customer special requests.

Cylinder and measuring point's number are shown in Fig. 2. Four measuring points according to the above principle are chosen in each cylinder. Two points of them are located near the machining face. The other two points are laid in the bottom of cylinder. There are totally sixteen points shown below as Figs. 3 and 4.

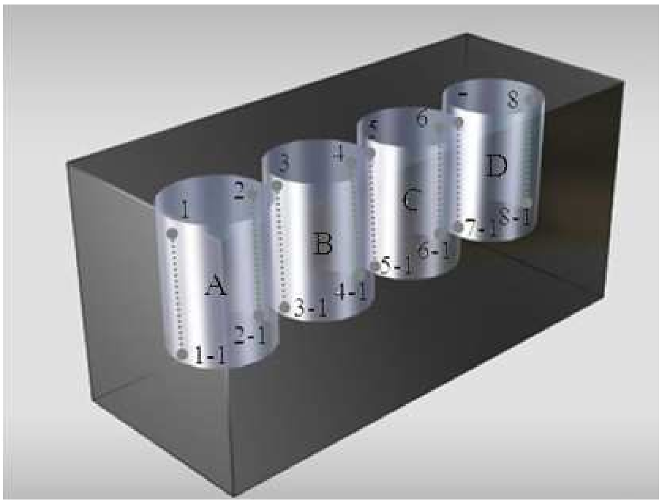

Fig. 2 Cylinder sketch and the measuring points

Fig. 3 Measuring points near top plane

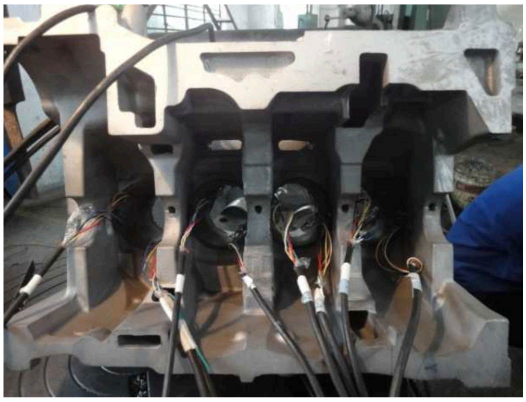

Fig. 4 Measuring points at bottom plane

Strain gage is protected by silica gel before grooving as shown in Fig. 5. The cylinder is grooved by triangle tool bit as presented in Fig. 6.

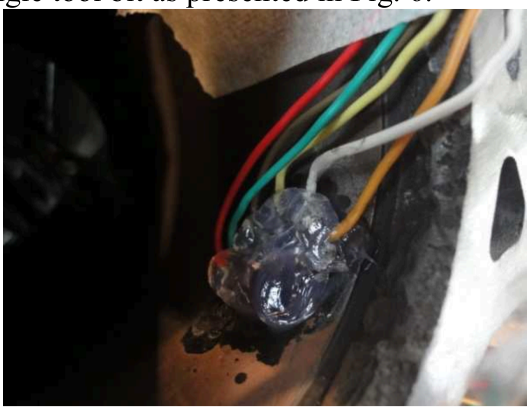

Fig. 5 Strain gage protected by silica gel

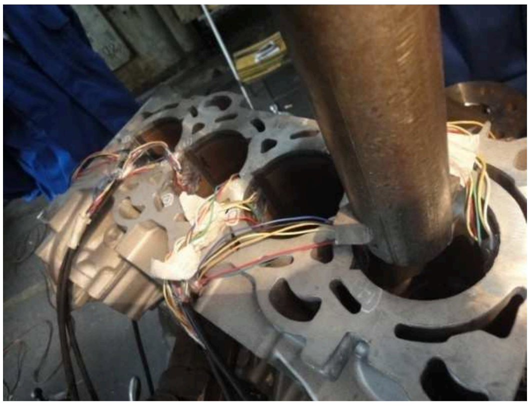

Fig. 6. Grooving with triangle tool bit

There are totally sixteen grooves in this experiment, which can be seen in Fig. 7.

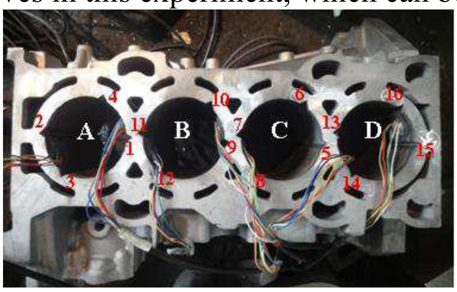

Fig. 7 Grooving order

4. Analysis of measuring result

4.1 Stress analysis

The maximum residual main stress σ_{max} is the major factor leading to structural damage. So a lot of work was unfolded to research and analyze work piece's σ_{max} at different measuring position. Testing results are shown in Table 1. Measuring result is contrasted from Fig. 8 and 10.

The number of residual stress in each side of top or bottom has decreased gradually in first three cylinders. Oppositely, this trend was moved towards the contrary direction: There is a rapid increase in the number of residual stress in cylinder D. The maximum value of the stress which obtained at the bottom of first groove in cylinder A achieves 264 MPa. Because the stress test in the bottom of the cylinder block is characterized for not being destructive by machining, the residual stress measured at bottom is greater than at top of the same cylinder A, as well as in the other cylinder.

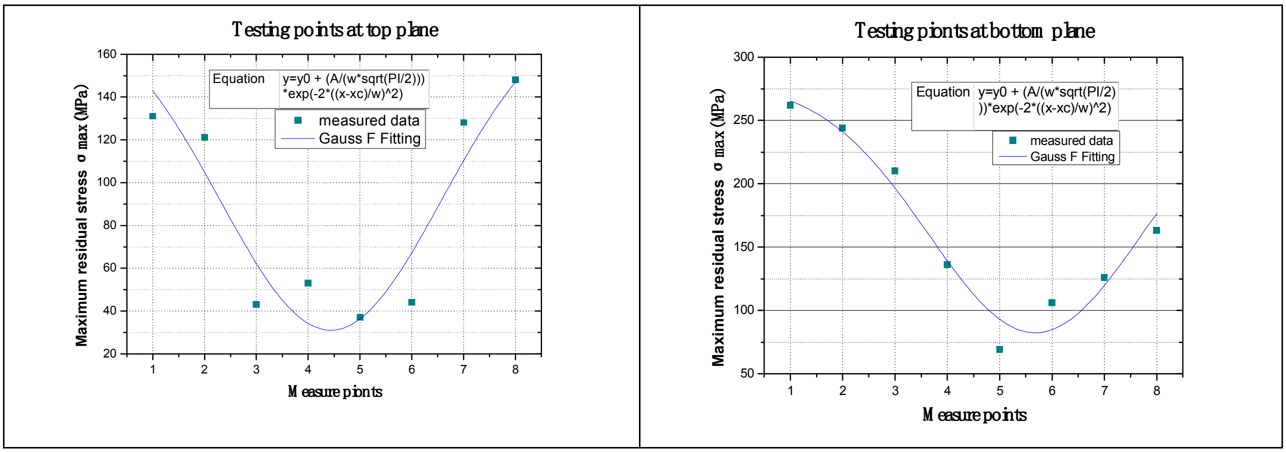

Fig. 8 Maximum main stress of measuring points

The maximum main stress at bottom testing points are considerably larger than that near the machined face in cylinder A which has the biggest difference for 167MPa at the same grooving position. It can be observed that the date of residual stresses at top plane is small than bottom plane with the exception of point 7, which corresponds to the last place for grooving destroy with the high degree of stress releasing. Measure points at top plane are totally smaller than points at bottom plane except for point 7. This phenomenon can be explained from the views of casting stress, microstructure and subsequent process. Firstly, the total solidification times of cylinder were 85s[19]. During this times, the solidification is firstly taken at the thin-wall thickness place of cylinder and its top, and then from the core of cylinder to its bottom, finally riser tube and runner. According to the way of progressive solidification, the effect of casting process leaded mould filling pouring from down to up, which bring about the temperature field cooling from down to top plane. Melt at top plane was solidified early and has good potential in ability of mold filling. After the middle of solidification stress at bottom side started to rise, this is largely because of limit of solidified metal at top of cylinder and the concretionary riser. Secondly, extensive metallographic indicated a significant refinement in microstructure at the top of the cylinder relative to the bottom[20]. This suggested an increase in alloy yield strength at the top of the cylinder relative to the bottom. In contrast, the coarse microstructure at the top of the cylinder likely resulted in a lower yield strength which allowed the residual stresses to exceed this yield strength. For this reason, stress relief was likely triggered more effectively at the top of the cylinder. Thirdly, Analysis supports that the stress on the surface has been released after machining, compared with bottom of cylinder where it with none machining process. As a result, the stress could be remained originally.

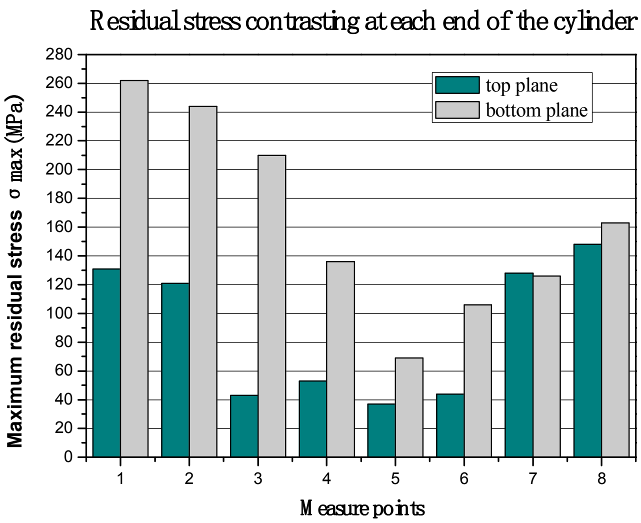

Fig. 9 Residual stress contesting at each end of cylinder

As shown in Fig. 9. It can be found that there are large stresses in cylinder A and D from the measurement results. σ_{max} of testing points 1-1, 2-1 and 3-1 in cylinder A exceeds 200MPa. There are also two reasons to explain this phenomenon. First of all, the cylinder internal is under pressure while the external side is under tension in the early time of solidification. In fact, external surface of aluminum ingots was under huge cold shock at early solidification process. Due to the thermal resistance of aluminum ingots, temperature at internal of aluminum ingots does not change. So the distribution of stresses is characterized by pressure inside and tension outside. But this phenomenon will develop to the opposite direction due to factors such as stress concentration. The biggest tensile stress is appeared in corner of aluminum ingots. Secondly, analysis suggests that the first groove is made in cylinder A which has large rigidity and restraint intensity due to little damage in the cylinder. Consequently, the great stress released from the groove. Cylinder D which is a last part that damaged by grooving releases larger stresses. That is why stress in cylinder A and D is larger than cylinder B and C.

5. Conclusion

In order to measure the residual stresses in fabric composite engine block whose material properties are heavily dependent on the relative location, a new measured method was devised. The residual stresses in fabric cylinder grooving method. From the comparison of the measured residual stresses with the thermal residual stresses calculated by numerical modeling, it was found that the new simple method estimated the residual stresses pretty well. Another advantage of the new method was that it was better than other methods like hole drilling method and sectioning method which is not convenient to use in the cylindrical work piece.

The observed variation in residual stress from top to bottom along the cylinder was likely the result of the mould geometry and cooling rate discrepancies during casting. Extensive metallographic indicated a significant refinement in microstructure at the bottom of the cylinder relative to the top, which occurred due to increased cooling rate at the bottom of the cylinder. In turn, this suggested an increase in alloy yield strength at the bottom of the cylinder relative to the top. This increased yield strength at the bottom of the cylinder likely reduced the susceptibility of the cylinder to rapid relief of residual stress at elevated temperature.

Values of stress in engine block were found to exceed the yield stress and approach its ultimate tensile strength. This suggested that a high build up of stress in the block, which may lead to dimensional distortion. Further investigation is warranted to characterize the residual stresses in the engine block following the T7 heat treatment process. The impact of variations in casting practice on grain size and stress level is envisaged for future studies.

Acknowledgements

This paper is sponsored by National Natural Science Foundation of China (51305253), Top Discipline Plan for Mechanical Engineering of Shanghai Municipal Education Commission (YLJX12-2) and Shanghai University of Engineering Science Science Innovation Found for Graduate Students (No.13KY502). The help extended by Shanghai Research & Development Center for Key Technologies of Intelligent Ultra-Intense Laser Processing Equipments is also sincerely acknowledged.

Reference

[1] H.T. Nguyen, Q.T. Chu, S.E. Kim. Fatigue analysis of a pre-fabricated orthotropic steel deck for light-weight vehicles J. *Journal of Constructional Steel Research.* 67(4) (2011) 647-655.

[2] Q. G. Wang. Latest advances and developments in aluminum shape casting J. *China Foundry.* 10(1) (2013) 43-49.

[3] M. Carboneras, L. S. Hernández, J. A. del Valle, *et al.*Corrosion protection of different environmentally friendly coatings on powder metallurgy magnesium J. *Journal of Alloys and Compounds.* 496(1-2) (2010) 442-448.

[4] Y. Xu, J. Kang, T. Huang ,*et al.* Thermal Stresses in a Cylinder Block Casting Due to Coupled Thermal and Mechanical Effects J. Tsinghua Sceince and Technology. 13(2) (2008) 132-136.

[5] H. Yamagata, W. Kasprzak, M. Aniolek, *et al.* The effect of average cooling rates on the microstructure of the Al–20% Si high pressure die casting alloy used for monolithic cylinder blocks J. Journal of Materials Processing Technology. 199 (2008) 84-90.

[6] J. L. Cavazos, R. Colás. Quench sensitivity of a heat treatable aluminum alloy J. Materials Science and EngineeringA. 363(1-2) (2003) 171-178.

[7] P. Barsanescu, P. Carlescu. Correction of errors introduced by hole eccentricity in residual stress measurement by the hole-drilling strain-gage method J. *Measurement.* 42(3) (2009) 474-477.

[8] J. W. Kim, D. G. Lee. Measurement of residual stresses in thick composite cylinders by the radial-cut-cylinder-bending method J. Composite Structures. 75 (2006) 261-266.

[9] K. Masláková, F. Trebuňa, P. Frankovský, *et al.* Applications of the Strain Gauge for Determination of Residual Stresses using Ring-core Method J. *Procedia Engineering.* 48(10) (2012) 396-401.

[10] R. Gou, Y. Zhang, X. Xu, *et al.* Residual stress measurement of new and in-service X70 pipelines by X-ray diffraction method J. *NDT & E International.* 44(5) (2011) 387-393.

[11] P. Angerer, W. Artner, E. Neubauer, *et al.* Residual stress in spark-plasma-sintered and hot-pressed tantalum samples determined by X-ray diffraction methods J. *International Journal of Refractory Metals and Hard Materials.* 26(4) (2008) 312-317.

[12] R. C. Wimpory, M. Boin. Emphasizing the accuracy of the uncertainty of residual stress determination using neutron diffraction J. *Procedia Engineering.* 10(8) (2011) 1639-1644.

[13] M. Kashefi, A. Rafsanjani, S. Kahrobaee, *et al.* Magnetic nondestructive technology for detection of tempered martensite embrittlement J. *Journal of Magnetism and Magnetic Materials.* 324(23) (2012) 4090-4093.

[14] A. Karabutov, A. Devichensky, A. Ivochkin, *et al.* Laser ultrasonic diagnostics of residual stress J. *Ultrasonics.* 48(6-7) (2008) 631-635.

[15] H. T. Lee, C. Liu. Optimizing the EDM hole-drilling strain gage method for the measurement of residual stress J. *Journal of Materials Processing Technology.* 209(15-16) (2009) 5626-5635.

[16] L. Álvarez, C. J. Luis, I. Puertas. Analysis of the influence of chemical composition on the mechanical and metallurgical properties of engine cylinder blocks in grey cast iron JComposite Structures. 153(10) (2004) 1044.

[17] S. M. Yoo, Y. S. Cho, C. C. Lee, *et al.* Optimization of Casting Process for Heat and Abrasion Resistant Large Gray Iron Castings J. *Tsinghua Science & Technology.* 13(2) (2008) 152-156.

[18] N. Hasebe, C. Bucher, R. Heuer. Heat conduction and thermal stress induced by an electric current in an infinite thin plate containing an elliptical hole with an edge crack J. *International Journal of Solids and Structures.* 47(1) (2010) 138-147.

[19] A. Çetin, and A. Kalkanli. Numerical simulation of solidification kinetics in A356/SiCp composites for assessment of as-cast particle distribution J. *Journal of Materials Processing Technology.* 209(10) (2009) 4795-4801.

[20] M. Merlin, G. Timelli, F. Bonollo, *et al.* Impact behaviour of A356 alloy for low-pressure die casting automotive whe*els J.* Journal of *Materials Processing Technology. 209(2*) (2009) 1073, 2009.